ʒ

# Spontaneous Dipole Alignment in Films of $N_2O$

Richard Balog, P. Cicman, N. C. Jones, and D. Field*

*Department of Physics and Astronomy, and Institute for Storage Ring Facilities, University of Aarhus, 8000 Aarhus C, Denmark*
(Received 11 June 2008; published 18 February 2009)

Experimental data obtained using low energy electron beams are presented which show that films of $N_2O$, of several hundred monolayers (ML), spontaneously acquire a positive potential of as high as 5 V. Films do not possess a dipole double layer but for $>40$ ML display a constant electric field within the material. This new phenomenon is attributed to dipole alignment. The phenomenon also shows a strong temperature dependence. This is revealed by the differing dependence of the surface potential on the film thickness at different temperatures and by electron transmission spectra which display marked structure at 62 K which is absent at 40 K.

A new phenomenon is reported here in which films of $N_2O$ deposited on gold spontaneously acquire positive potentials at the film-vacuum interface with respect to the film-metal interface. Potentials can be as high as several volts depending on film thickness, and the behavior shows a strong temperature dependence, especially for thin films. No charge transfer is observed to occur at the metal-$N_2O$ boundary and surface potentials are found to increase smoothly with film thickness. This behavior is in marked contrast to the well-known formation of potentials by layers of organic semiconductors [1–8] in which in all cases, save the single exception of $Alq_3$ [7], the whole potential change occurs within the first few layers near the interface through charge transfer or by self-assembly of adsorbed molecules of high dipole moment.

Our experiments are conducted by irradiating a film of $N_2O$ with low energy, high resolution electron beams using currents of typically 200 fA. A schematic diagram of the UHV apparatus, base pressure $\sim 10^{-10}$ mbar, is shown in Fig. 1 with the sample in position for electron irradiation. Electrons are formed through threshold photoionization of 99.9999% argon at 15.76 eV using synchrotron radiation from the undulator beam line on the ASTRID storage ring at Aarhus [9,10]. Photoelectrons have an energy resolution which is determined by the energy resolution in the photon beam, set here to $\sim 1.6$ meV full-width half-maximum. Electrons are formed into a beam and focused by a 4-element electrostatic zoom lens, impinging on a Au substrate with a spot size of diameter 2 to 3 mm depending on the electron energy. The current at the Au substrate is measured using a femtoammeter (Keithley 6430). All surfaces S1–L4, $V_{cc}$, and $S$ are spray coated with Acheson Aerodag $G$ graphite. The apparatus is enclosed in a double mu-metal shield to exclude the magnetic field of the Earth or other stray fields. The pressure in the apparatus with argon present is a few times $10^{-7}$ mbar.

The Au substrate is in the form of a 750 nm thick layer of polycrystalline material on Ta, grain size $<100$ nm. The substrate is cooled with a He cryo-cooler to temperatures in the range of 35 K upwards. The gold surface is cleaned by resistive heating to 750 K. Standard dosing techniques from the background gas allow the deposition of films of a known number of monolayers (ML), where 1 ML $= 10^{15}$ molecules/$cm^2$. The rate of deposition was $\sim 0.5$ ML per second, calibrated using temperature programmed desorption. $N_2O$ films are grown in dark conditions. Absolute errors in quoted film thicknesses are typically 30%.

The energy of the electrons emerging from the L1–L4 lens is given by the potential difference between their point of formation, at the center (S2) of the photoionization region, and the potential on the last lens element, L4, electrically connected to the final aperture contiguous
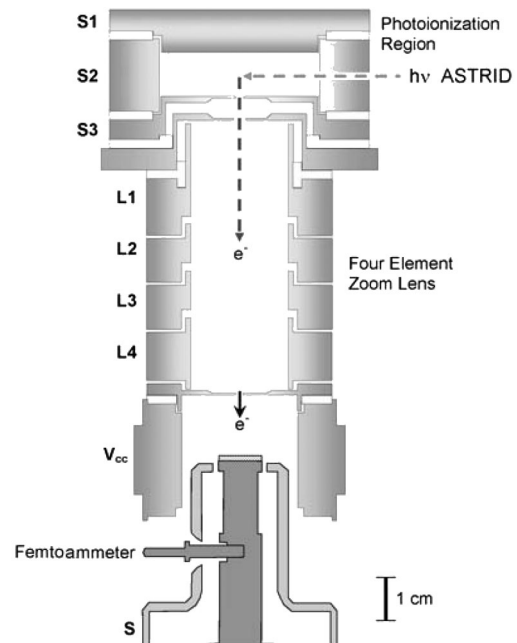


FIG. 1. A scale diagram of the apparatus. Monochromatic synchrotron radiation, $h\nu$ ASTRID, enters a photoionization source containing argon. Photoelectrons, expelled by a weak electric field, are focused onto a film of $N_2O$.

with it. This energy is typically set to a nominal value of 1 eV. The energy of electrons arriving at the target is defined by the potential difference at vacuum between S2, where the electrons are formed, and the sample. This energy can be varied by applying a variable offset potential to all elements S1 to L4 with respect to the Au substrate. The value of the offset potential associated with the inception of the transmitted current, corresponding to zero energy electrons, represents the difference in work function of the materials involved. Here for clean Au and graphite on S2 we have measured a value of ~0.2 eV. The change of potential at the surface associated with $N_2O$ adsorption is then obtained by measuring the potential associated with the inception of the current. All recorded values of surface potential for $N_2O$ films are relative with respect to the clean Au substrate.

The electron currents used in our experiments are 3 to 4 orders of magnitude lower than those used in earlier studies of the interaction of electron beams with solids. Our energy sweep times are typically an order of magnitude longer. Thus the total dose of electrons to the sample in a scan is 2 to 3 orders of magnitudes or more lower than in any previous work on electron-solid interactions.

The spontaneous surface potential at the $N_2O$-vacuum interface acquired by films of different thickness and laid down at different temperatures is shown in Fig. 2. The general characteristics of the data are the following. (i) For films above a thickness of 40 ML there remains a constant electric field within the film. There are data to 540 ML at 62 K which continue this trend. (ii) For the thickest films spontaneous charging is greater for lower temperatures. (iii) For thinner films, the inset to Fig. 2 shows that the surface potential displays quite different behavior than for thick films with respect to the temperature at which films were formed. Thin 52 K films display
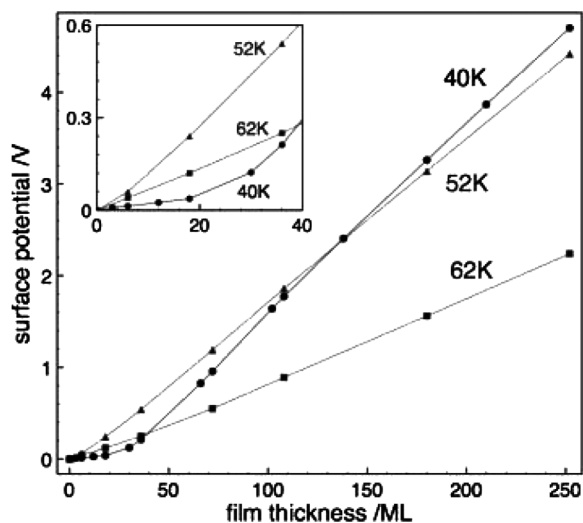
the steepest rise with film thickness, followed by the 62 K data, the latter overtaken by the 42 K data at 30 ML.

Separate electron transmission experiments through films of $N_2O$ were also performed. Figure 3 shows data for 108 ML films at 40, 52, and 62 K, displaced vertically for clarity. The 40 K data resemble a clean Au surface, the 52 K data show a weak feature at 2 eV, and the 62 K data show a strong feature at ~0.8 eV. Evidently the spectra in Fig. 3 are not associated with a molecular but rather with a structural characteristic. A succession of such spectra was obtained at each temperature for different film thicknesses. At both 52 K and 62 K, the dip position increases in energy with film thickness and reveals a very clear 1:1 correspondence with the surface potential. This is shown for 62 K data in Fig. 4.

In addition to the observations presented in Figs. 2–4, we have investigated the reversibility of spontaneous charging with respect to temperature. For thin films, below 20 ML, deposited at 40 K and then heated to 62 K, the surface potential increases from close to zero to the value obtained by direct deposition at 62 K, reflecting results shown in the inset to Fig. 2. For thicker films of 180 ML and 230 ML deposited at 40 K, warming to 62 K causes a drop in surface potential, again as data in Fig. 2 would suggest. However, the drop in surface potential is only 409 mV for the 180 ML layer and 600 mV for the 230 ML layer, whereas data in Fig. 2 indicate values of 1.5 to 2 V. This suggests that only partial relaxation of structure occurs by thermal excitation of thick layers. We conclude that once structure is locked into the system, there is a barrier to its removal for thick films but not for thin films. Similar experiments, but involving cooling of films, show no effect on the surface potential or on the transmission spectra of the films involved, for all measured thicknesses.
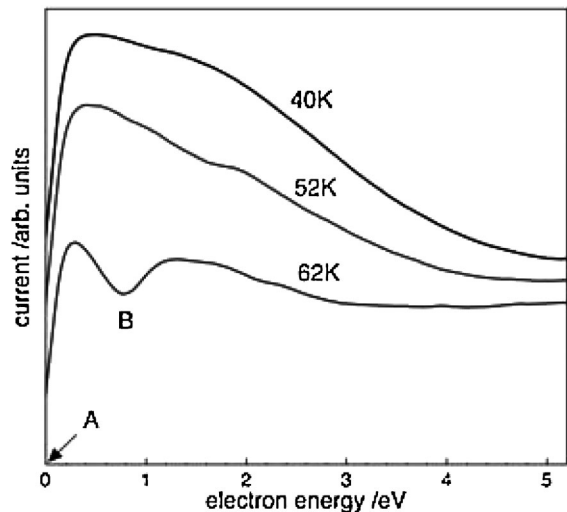


FIG. 2.   Measured surface potentials as a function of $N_2O$ film thickness. Films are deposited at 40, 52, and 62 K. Inset: detailed view for thicknesses below 40 ML.



FIG. 3.   Electron transmission spectra for 108 ML $N_2O$ films deposited at different temperatures displaced for clarity. Point A (see text and Fig. 5) lies at zero energy, and point B at the energy of the dip potential. Maximum currents are ~200 fA.
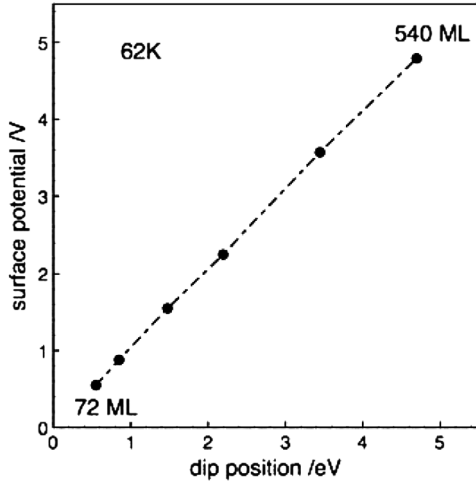
FIG. 4. Relationship between position of dips in electron transmission spectra and observed surface potentials. See Fig. 3.

We now show that spontaneous charging may result from dipole alignment within the film, restricting our discussion to films of thickness >40 ML. As the authors in [7] note for the case of $Alq_3$ films, the linearity of growth of potential indicates no net charge within the film and a constant surface polarization $P$. The electric field arises from 4.8 V over 210 ML (see Fig. 2) at 40 K, that is, $6.404 \times 10^7$ V/m for an intermolecular periodic distance of 3.6 Å. This yields $P = 1.13 \times 10^{-3}$ C/m² [7]. This may be compared with the surface polarization that would arise from perfect alignment of the $N_2O$ dipoles. The latter is the polarization essentially inherent in a single molecule and is given by the gas phase dipole moment, $\mu$, corrected for depolarization, divided by the volume of the molecule. The corrected dipole moment, $\mu_{corr}$, is given by [11] and references therein as

$$\mu_{corr} = \frac{\mu}{1 + \frac{\alpha k}{a^3}}, \tag{1}$$

where $\alpha$ is the gas phase polarizability of $N_2O$ ( = $3.31 \times 10^{-30}$ m³), $k \sim 10$, and $a = 3.6$ Å. This yields $\mu_{corr} = 0.097$ D. The volume of the molecule may be estimated either through the known polar surface area of 56.46 Å² or by using a surface area of $10^{-15}$ cm² and a spacing of 3.6 Å, giving the same result within 5%. Perfect alignment then yields a surface polarization of $8.6 \times 10^{-3}$ C/m². Comparison with the observed value of $1.13 \times 10^{-3}$ C/m² yields ~13% of perfect alignment. It is therefore feasible that dipole alignment can yield the observed surface charging. We note that the effective dipole moment of $N_2O$ may be modified by the presence of both polar and nonpolar dimers within the solid [12].

To explain our results, we propose that the energy bands of $N_2O$ films change linearly with increasing film thickness. As layers are added (say at 62 K), the effective work function drops. The potential at the surface-vacuum inter-

face is effectively drawn towards lower energy by a value equal to the observed potential and thus increasingly for thicker layers (Fig. 5).

We turn now to the 62 K data in Fig. 3. Let us add layers until we are at point A in Fig. 5. If we now perform a transmission experiment, from the point A where the potential between S2 and the sample is zero, the current rises first to a maximum value. Beyond this maximum, the increasing energy of the electrons results in more efficient backscattering. Hence the measured current falls towards B. Note that the electrons penetrate the $N_2O$ but cannot reach the metal because there is a band gap, given the ideal case of an absence of band gap states. The measured current between points A and B is then an induction (or displacement) current. However, when the electron energy has risen to the value at B, electrons have enough energy to penetrate fully through the layer and reach the metal. Thus some of the electrons which at lower energy were backscattered from within the film can now pass into the metal. The net result is an increase in current. This forms the dip observed. To explain our result in Fig. 4 that the surface potential is equal to the position of the dip, this model requires that the bottom of the conduction band is very close to the vacuum level. The absence of the dip at 40 K and its relative weakness at 52 K compared with 62 K, Fig. 3, may arise from different structural characteristics of the $N_2O$ film, discussed below, leading to different electron transmission and scattering properties.

In Fig. 5, the Fermi level of the film is shown as falling as film thickness increases. This is necessary to explain why the surface potential continues to increase linearly with film thickness without apparently saturating, as seen for the thick films in Fig. 2. The same situation holds for $Alq_3$ films, and we come to the same conclusion as in [7] that the system is not at thermodynamic equilibrium since equilibrium requires that the Fermi level maintains a constant value throughout the entire system. At greater layer
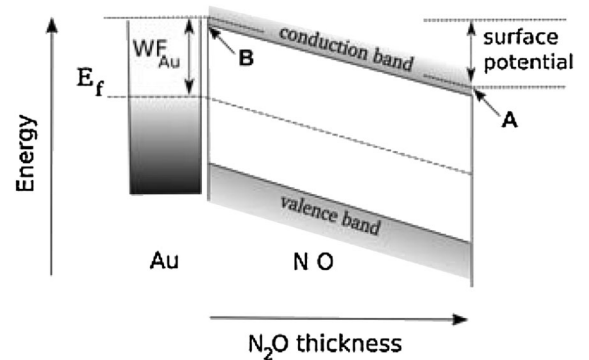


FIG. 5. Schematic of the energy bands of the Au-$N_2O$ film system. $E_f$ is the Fermi level of the Au, and $WF_{Au}$ is the clean Au work function. Valence and conduction bands of the $N_2O$ film are also shown. The significance of A and B is described in the text.

thicknesses, the surface potential may exceed the work function of Au. Spontaneous electron emission from the metal can then lead to a limit on the surface potential. Accompanying this, there may result a transition to normal dielectric behavior in thick films as the passage and trapping of electrons disrupt the dipole alignment.

An alternative interpretation of our transmission data is that transmission spectra at 62 K represent the superposition of two spectra. One spectrum arises from zones of surface polarized material, and the other from zones of either unpolarized material without dipole alignment or bare metal. The latter would suppose the formation of isolated columns of $N_2O$.

A tentative explanation of the anomalous behavior of the system for thin films, shown in the inset to Fig. 2, is as follows. At 40 K, $N_2O$ is crystalline with no net dipole in the unit cell [13,14]. Thus crystalline $N_2O$ should show no macroscopic dipole alignment. Up to 20 ML, this is observed at 40 K. We postulate that amorphous $N_2O$ then forms for thicker layers and that this amorphous structure prefers a partially dipole aligned configuration. At 52 K, $N_2O$ shows only a small propensity to be crystalline and tends to the amorphous phase with a partial dipole alignment, but to a slightly lesser extent than at 40 K. At 62 K, films are wholly amorphous but show more thermally perturbed alignment. With regard to thermal perturbation, films evaporate at $\sim 80$ K.

Whatever the structure of the $N_2O$ films, the use of large doses of charge could wipe out the spontaneous creation of surface potential if electrons are trapped at the surface. To investigate this we irradiated a surface of a 540 ML film, prepared at 60 K, for a period of 1800 seconds with a current of 200 fA at a nominal energy of 300 meV. This yielded a total dose of $\sim 5.1 \times 10^{-5}$ C/m$^2$. The surface was observed to shift 200 mV less positive. The charge delivered is 11.7% of the total spontaneous polarization. Therefore the maximum possible shift should be 11.7% of the total surface potential of 4.8 V for this film, that is, 560 mV, if all charge accumulates at the surface and is sufficiently mobile to neutralize the surface polarization. Electrons at 300 meV penetrate the film but encounter the band gap and are therefore unable to reach the film-metal interface. They are multiply scattered and return towards the film-vacuum interface as described above. At the surface they are attracted by the positive charge and partially neutralize it.

In conclusion our experiments have revealed a novel phenomenon in thin films. Dipole alignment would appear to be a natural explanation for our observations of high surface polarization, but raises questions regarding the order in $N_2O$ films. Theory would be valuable to examine our somewhat speculative interpretation of the data but must be able to cope with weak long-range anisotropic interactions. We add that fluorobenzene, acetic acid, and water ices do not show the phenomenon described here. The reason may be that order is dictated in these species by hydrogen bonding and that this overwhelms dipole alignment. In future work we plan to investigate other species than $N_2O$ to discover if the phenomenon may be associated with a specific class of molecules.

*Corresponding author.
dfield@phys.au.dk

[1] A. Vilan, A. Shanzer, and D. Cahen, Nature (London) **404**, 166 (2000).

[2] K. Demirkan, A. Mathew, C. Weiland, Y. Yao, A.M. Rawlett, J.M. Tour, and R.L. Oplia, J. Chem. Phys. **128**, 074 705 (2008).

[3] U. Zerweck, Ch. Loppacer, T. Otto, S. Grafstrom, and L.M. Eng, Nanotechnology **18**, 084 006 (2007).

[4] I.H. Campbell, S. Rubin, T.A. Zawodzinski, J.D. Kress, R.L. Martin, D.L. Smith, N.N. Barahkov, and J.P. Ferraris, Phys. Rev. B **54**, R14321 (1996).

[5] J.X. Tang, C.S. Lee, and S.T. Lee, J. Appl. Phys. **101**, 064 504 (2007).

[6] M. Gratzel, Nature (London) **414**, 338 (2001).

[7] H. Ishii, N. Hayaski, E Ito, Y. Washizu, K. Sugi, Y. Kimura, M. Niwano, Y. Ouchi, and K. Seki, Phys. Status Solidi A **201**, 1075 (2004).

[8] H. Yamane, H. Fukugawa, S. Kera, K.K. Okudaira, and N. Ueno, J. Appl. Phys. **99**, 093 705 (2006).

[9] D. Field, N.C. Jones, S.L. Lunt, and J.-P. Ziesel, Phys. Rev. A **64**, 022708 (2001).

[10] S.V. Hoffmann, S.L. Lunt, N.C. Jones, D. Field, and J.-P. Ziesel, Rev. Sci. Instrum. **73**, 4157 (2002).

[11] A. Natan, L. Kronik, H. Haick, and R.T. Tung, Adv. Mater. **19**, 4103 (2007).

[12] M. Dehghani, M. Afshari, Z. Abusara, N. Moazzen-Ahmad, and A.R.W. McKellar, J. Chem. Phys. **126**, 164 310 (2007).

[13] S.I. Kovalenko, E.I. Indan, A.A. Khudotyoplaya, and I.N. Krupskii, Phys. Status Solidi A **20**, 629 (1973).

[14] A.A. Solodovnik and V.V. Danchuk, J. Low Temp. Phys. **122**, 493 (2001).